

Spin-orbit configuration interaction study of potential energy curves and transition probabilities of the mercury hydride molecule and tests of relativistic effective core potentials for Hg, Hg⁺, and Hg²⁺

Aleksey B. Alekseyev, HeinzPeter Liebermann, Robert J. Buenker, and Gerhard Hirsch

Citation: *The Journal of Chemical Physics* **104**, 4672 (1996); doi: 10.1063/1.471162

View online: <http://dx.doi.org/10.1063/1.471162>

View Table of Contents: <http://scitation.aip.org/content/aip/journal/jcp/104/12?ver=pdfcov>

Published by the AIP Publishing

Articles you may be interested in

Relativistic potential energy surfaces of XH₂ (X=C, Si, Ge, Sn, and Pb) molecules: Coupling of 1 A₁ and 3 B₁ states

J. Chem. Phys. **104**, 7988 (1996); 10.1063/1.471515

Geometric phase effects in H+O₂ scattering. II. Recombination resonances and statetostate transition probabilities at thermal energies

J. Chem. Phys. **104**, 7502 (1996); 10.1063/1.471461

Ab initio configuration interaction calculations of the potential curves and lifetimes of the lowlying electronic states of the lead dimer

J. Chem. Phys. **104**, 6631 (1996); 10.1063/1.471357

Theoretical study of potential energy surfaces for interactions of Pd₂ with CO

J. Chem. Phys. **104**, 1471 (1996); 10.1063/1.470912

Potential curves and transition moments of HGZN

AIP Conf. Proc. **216**, 417 (1990); 10.1063/1.39893



Spin-orbit configuration interaction study of potential energy curves and transition probabilities of the mercury hydride molecule and tests of relativistic effective core potentials for Hg, Hg⁺, and Hg²⁺

Aleksey B. Alekseyev,^{a)} Heinz-Peter Liebermann, Robert J. Buenker,
and Gerhard Hirsch

Bergische Universität-Gesamthochschule Wuppertal, Fachbereich 9-Theoretische Chemie, Gausstr. 20,
D-42097 Wuppertal, Germany

(Received 7 August 1995; accepted 11 December 1995)

Ab initio CI calculations have been carried out for the low-energy states of the mercury hydride molecule HgH and its isotopomers. A relativistic effective core potential (RECP) given by Ross *et al.* [J. Chem. Phys. **93**, 6654 (1990)] is employed to describe all but the Hg 5*d* and 6*s* valence electrons. Tests for a series of low-lying states of Hg, Hg⁺, and Hg²⁺ demonstrate that 0.1 eV accuracy is obtained at the SCF level with a high-quality basis set for this RECP in comparison with all-electron Dirac-Fock results up to 32 eV excitation energy. The DF values are themselves in error by 1–3 eV on the average compared to experiment, but the present CI calculations based on this RECP lead to considerably higher accuracy because of the importance of correlation effects in such determinations. Energy differences (12 cases) between states with the same number of electrons are computed to an accuracy of 0.1–0.2 eV in all cases after the spin-orbit interaction is included. These results compare favorably with those obtained by Häussermann *et al.* [Mol. Phys. **78**, 1211 (1993)] with a $\cdots 5s^2 5p^6 5d^{10} 6s^2$ RECP and a corresponding larger AO basis to describe the more tightly bound electrons. Good agreement is found for the spectroscopic constants of the HgH molecule in its lowest four electronic states: $X^2\Sigma^+_{1/2}$, $A_1^2\Pi_{1/2}$, $A_2^2\Pi_{3/2}$, and $B^2\Sigma^+_{1/2}$ (maximal errors of 1000 cm⁻¹ for T_e , 0.03 Å for r_e and 150 cm⁻¹ for ω_e). An RKR curve reported for the A_1 state is shown to be in error beyond $r=4.0 a_0$ because of its failure to describe a key avoided crossing with the B state. Radiative lifetimes computed for the $A^2\Pi$ multiplets are both found to agree with values deduced from experiment to within 40%. The calculations find no difference in the HgH and HgD radiative lifetimes for either the A_1 or the A_2 states, whereas a large distinction in the measured A_1 lifetimes of the two isotopomers is observed, thereby supporting the previous experimental conclusion that strong predissociation occurs in the HgH A_1 state. Numerous higher-lying electronic states are also studied, with T_e values up to 60 000 cm⁻¹, and on this basis it is argued that earlier assignments for the HgH $C-X$ and $D-X$ transitions are incorrect, as previously concluded by Nedelec *et al.* [Chem. Phys. **134**, 137 (1989)]. © 1996 American Institute of Physics. [S0021-9606(96)00411-4]

I. INTRODUCTION

As pointed out by Stwalley in 1975,¹ “HgH has had a rich history during the development of molecular spectroscopy.” Indeed, the very first observation of the HgH spectrum was reported by Eder and Valenta² and dates back to 1894. In 1925–1928 Hulthén³ performed the first thorough rotational analysis of these bands and correctly assigned them to transitions from the three lowest excited states, $A_1^2\Pi_{1/2}$, $A_2^2\Pi_{3/2}$, and $B^2\Sigma^+$, to the ground $X^2\Sigma^+$ state by applying Hund’s theory of molecular spectra. This analysis was extended and improved in the following decade by Rydberg⁴ and Fujioka and Tanaka.⁵ In order to determine potential curves for the HgH ground and excited states and obtain their spectroscopic constants, Rydberg employed an approach which has subsequently come to be known as the Rydberg–Klein–Rees (RKR) method. He has also found evidence for two more $^2\Sigma^+$ states, C and D . Further analysis of

the HgH spectra was done in the sixties by Porter, Davis, Phillips, and Eakin.^{6–9} It became possible in their work to achieve higher resolution and to assign additional spectral bands which allowed term values of a larger number of vibrational levels to be determined, e.g., the energies of the highest vibrational levels of the $X^2\Sigma^+$ ground state which have been observed to date: $v''=4$ for HgH and $v''=5$ for HgD.

Later experimental studies^{10–13} concentrated mainly on radiative lifetime measurements for a number of rovibrational levels of the $A_1^2\Pi_{1/2}$ and $A_2^2\Pi_{3/2}$ states in the HgH and HgD molecules. In addition, Dufayard *et al.*^{12,13} have carried out a detailed analysis of the $A_1^2\Pi_{1/2}$ state predissociation caused by a crossing with the inner limb of the $X^2\Sigma^+$ potential curve, an effect which has a crucial influence on the lifetimes of the vibrational levels of the upper state. It should also be noted that for some time the $X^2\Sigma^+$ ground state of HgH has attracted some special attention for two reasons: First, it possesses a fairly deep minimum ($D_0^0=0.3744$ eV as determined by Stwalley¹), contrary to what one would expect

^{a)}On leave from the Institute of Physics, St. Petersburg State University, 198904 St. Petersburg, Russia.

on the basis of a purely van der Waals type interaction. This was explained by Mulliken¹⁴ as the result of the interaction between the two configurations which characterize the lowest $^2\Sigma^+$ states dissociating to the 1S and 3P Hg atom states, respectively. Second, this state is considered to be a classic example of rotational predissociation, and has been analyzed accordingly by both Herzberg¹⁵ and Stwalley.¹ In spite of this long and impressive history of experimental investigations, however, vibrational frequencies, equilibrium bond distances and excitation energies are only known for the lowest four HgH states: $X\ ^2\Sigma^+$, the two strongly split components of $A\ ^2\Pi$, and $B\ ^2\Sigma^+$. Rotational constants have also been reported¹⁶ for two other $^2\Sigma^+$ states (C, D), with ν_{00} values relative to $X\ ^2\Sigma^+$ of up to 37 000 cm⁻¹, although this assignment has been questioned in more recent work.¹³

In the last 20 years it has become feasible to carry out accurate nonempirical calculations which predict details of the electronic spectra of such heavy systems, both with all-electron methods^{17,18} and with the aid of relativistic effective core potentials (RECPs).¹⁹ The HgH molecule has drawn fairly strong attention from theoreticians involved in developing these methods, probably because it represents a major challenge for an accurate *ab initio* approach. Five such calculations of HgH have been done up to now, all of them employing a core potential method. The main goal of these studies was to calculate potential energy curves and spectroscopic constants of the four lowest HgH states observed experimentally. The early studies of Das and Wahl²⁰ and Hay *et al.*²¹ had to overcome difficulties in constructing adequate core potentials for the mercury atom, a procedure which was not at all well established at that time, as well as in carrying out a suitably accurate CI treatment. In the later studies of Bernier *et al.*²² and Dolg *et al.*²³ only three outer electrons were included in the valence shells treated explicitly, which is probably too rough an approximation to accurately describe this system. The most sophisticated and consistent calculation of HgH was recently reported by Häussermann *et al.*,²⁴ who treated 20 Hg electrons in the valence shell. However, these authors concentrated mainly in their study on testing the accuracy of the RECP method in comparison with the all-electron approach in calculations of the mercury atom and its singly and doubly charged positive ions.

In our laboratory RECP calculations have been carried out in the last few years for a number of diatomic molecules containing similarly heavy atoms such as bismuth^{25–29} and thallium.³⁰ The basic technique employed is a spin-orbit configuration interaction treatment based on the Λ - S eigenfunctions obtained from conventional CI calculations which neglect spin-dependent interactions. As such it is very similar to the CIPSO method,³¹ also tested in Ref. 24, and to the relativistic CI approach of Balasubramanian, Pitzer and co-workers.³² Potential energy curves and radiative lifetimes have been computed in our work for a large number of electronic states for such systems as BiH,²⁵ BiF,²⁶ BiO,²⁷ Bi₂,²⁸ and BiI²⁹ as well as for related compounds of the lighter antimony atom.^{33–35}

In the present study spin-orbit CI calculations have been carried out employing the mercury atom RECP of Ross

*et al.*³⁶ which is similar in nature to those used in our earlier work with bismuth, thallium, and antimony compounds.^{25–29,33–35} The main goal is to overcome shortcomings of previous theoretical studies and to obtain spectroscopic constants for the lowest-lying electronic states of the HgH molecule, some of which have yet to be completely characterized experimentally. In addition to the relevant potential energy curves, transition probabilities have also been obtained for a number of key radiative processes, particularly the depopulation of the $A_1\ ^2\Pi_{1/2}$ and $A_2\ ^2\Pi_{3/2}$ states for which lifetime measurements are available.^{10–13} Before discussing these results, however, we shall consider a series of related computations for the Hg, Hg⁺, and Hg²⁺ atomic species which can be compared with the benchmark results for the same systems obtained by employing a variety of theoretical methods, as reported by Häussermann *et al.*²⁴

II. DETAILS OF THE CALCULATIONS

The basic approach employed in the present theoretical treatment is a spin-orbit CI based on relativistic effective core potentials (RECPs) for the mercury atom. The RECP of Ross *et al.*³⁶ used in this study is of the semicore variety, with the Hg 5*d* and 6*s* electrons in the active MO set (thirteen such electrons for HgH). Comparison will also be made with the pseudopotential calculations of Häussermann *et al.*²⁴ which add the 5*s*, 5*p* electrons to the active set. Several AO basis sets are considered for the purpose of carrying out test calculations for the mercury atom and its positive ions, the first of which is later employed for the description of mercury hydride. It is referred to as Basis I and is also taken from the work of Ross *et al.*,³⁶ a 3*s*3*p*4*d* primitive set of Cartesian Gaussians, but augmented by diffuse *s* ($\alpha=0.01\ a_0^{-2}$) and *p* ($\alpha=0.012\ a_0^{-2}$) functions for the purpose of obtaining an adequate representation of the Rydberg states of HgH and the mercury atom itself. In the atomic calculations an additional diffuse *d* function ($\alpha=0.020\ a_0^{-2}$) has been included to obtain a better description of the second Hg⁺ 2D state. The corresponding H atom basis is taken from Dunning³⁷ and consists of a 5*s* set of primitives contracted to 3*s* and augmented by a single *p* function with an exponent of $0.75\ a_0^{-2}$. Consistent with previous work, an SCF calculation is carried out at each bond distance considered, in this case for the $^2\Sigma^+$ Λ - S ground state of HgH ($\cdots 2\sigma^2 3\sigma$, where $1\sigma^2 1\delta^4 1\pi^4$ electrons corresponding to the 5*d*¹⁰ shell of Hg are omitted in the present notation).

The same RECP and AO basis are also employed for atomic calculations in order to compare with the corresponding benchmark data of Häussermann *et al.*²⁴ Two additional basis sets have been considered for this purpose. Basis II consists of an (8*s*8*p*7*d*) primitive set for mercury, contracted to [6*s*6*p*4*d*], and augmented with single diffuse functions of *s*, *p*, and *d* type and two *f*-type polarization functions.²⁴ Another basis set (III) is adapted from the (21*s*19*p*16*d*9*f*) all-electron basis set given in the same reference²⁴ by removing functions with large exponents which primarily serve to describe inner shells of mercury not included in the Ross *et al.* RECP³⁶ employed in the present

TABLE I. Technical details of the MRD-CI calculations of HgH.^a

C_{2v} symm.	$N_{\text{ref}}/N_{\text{root}}$	SAFTOT/SAFSEL	$C_{\infty v}$ notation	Σc_p^2
$^2B_{1,2}$	89/6	2 843 499/18 719	$1^2\Pi$	0.9476
			$2^2\Pi$	0.9478
2A_1	124/6	3 056 385/22 929	$1^2\Sigma^+$	0.9435
			$2^2\Sigma^+$	0.9428
2A_2	91/6	3 552 717/24 185	$1^2\Sigma^-$	0.9423
			$2^2\Sigma^-$	0.9186
$^4B_{1,2}$	82/6	2 805 880/22 121	$1^4\Pi$	0.9498
			$2^4\Pi$	0.9514
4A_1	90/6	2 628 963/26 932	$1^4\Sigma^+$	0.9481
			$2^4\Sigma^+$	0.9470
4A_2	86/6	3 325 840/25 514	$1^4\Sigma^-$	0.9379
			$2^4\Sigma^-$	0.9138

^aThe number of selected SAFs and the Σc_p^2 values over reference configurations (for the lowest roots of each symmetry) are given for $r=3.4a_0$. SAFTOT designates the total number of generated, SAFSEL the number of selected SAFs, N_{ref} and N_{root} refer to the number of reference configurations and roots treated, respectively.

work. The resulting primitive set is $(9s9p8d4f)$, but it is also augmented with a diffuse p function ($\alpha=0.012 a_0^{-2}$) to provide a better description of the P states of the Hg atom and ions, particularly the 1P state of the neutral atom.

In the HgH calculations the SCF-MOs transform according to $C_{\infty v}$ linear irreducible representations, but the theoretical treatment itself is carried out in the C_{2v} subgroup. Similarly the mercury atom AOs have proper spherical symmetry, but the corresponding calculations with them are also carried out in the C_{2v} subgroup. In all cases these orbitals serve as an orthonormal one-electron basis for the standard MRD-CI technique with configuration selection and energy extrapolation.³⁸ Perturbative energy corrections of two types are considered, including the generalized version of the Davidson–Langhoff correction.^{39,40} The Λ – S energy results obtained at this level of treatment have been found to agree with corresponding full CI benchmark data to within 1–2 kcal/mol for a large series of test systems with a similar number of active electrons in their respective theoretical treatments.⁴¹ The Table CI algorithm⁴² is employed in the MRD-CI calculations for efficient handling of the complex open-shell relationships which arise from an unrestricted choice of reference configurations from which all singly and doubly excited spin-adapted functions are generated. All 12 outer electrons of the mercury atom are included in the CI active space. Details concerning sizes of reference sets and numbers of roots treated in each Λ – S space for HgH are given in Table I, along with the dimensions of the corresponding generated and selected MRD-CI spaces. The $C_{\infty v}$ notation of the lowest roots is also given, as well as the corresponding sum value for the squares of the coefficients of all reference configurations in the final CI wave functions ($r=3.4 a_0$), which quantity appears explicitly in the generalized Davidson–Langhoff correction formula.^{39,40} Six roots have been obtained for the quartet and doublet multiplicities of each of the four C_{2v} representations at each bond distance considered. A selection threshold value of $T=5.0 \mu E_h$ has been employed throughout. The truncated CI wave functions

are subsequently employed to compute matrix elements between corresponding electronic states, primarily for electric dipole transition moments and the spin–orbit operator. An analogous CI treatment has also been carried out for the mercury atom and its first two positive ions which is based on the SCF-AOs of the $\cdots 5d^{10}6s^2^1S_g$ ground state of the neutral system.

The next step in the theoretical treatment is a spin–orbit CI in a basis of the Λ – S eigenfunctions multiplied with appropriate spin functions. More details for such odd-electron relativistic CI calculations may be found in our previous work,²⁷ and more general information is given in Refs. 25 and 26. The secular equations so defined are of order 72. Two such CI calculations are carried out for degenerate partners (Kramers’ theorem), leading to exactly the same energy eigenvalues but to distinct pairs of eigenfunctions which are needed for the computation of perpendicular transition moments.²⁷ The appropriate estimated full CI Λ – S energies are placed on the diagonal of the CI matrix, whereas the off-diagonal (spin–orbit) matrix elements are obtained by employing the truncated versions of the Λ – S CI eigenfunctions. Calculations are carried out at intervals of 0.05–0.1 a_0 for $r=2.5$ –50 a_0 , then with larger increments up to $r=18.0 a_0$ to simulate HgH dissociation. Again a similar treatment has been carried out for the mercury atom and its positive ions.

Finally, the resulting spin–orbit CI potential energy curves have been fit to polynomials and substituted in one-dimensional nuclear motion Schrödinger equations.^{43,44} The eigenfunctions obtained are then combined with the transition moment results for the electronic spin–orbit CI wave functions to obtain transition probabilities for various pairs of vibrational states. Einstein coefficients of spontaneous emission are computed on this basis, as well as radiative lifetimes for individual vibrational levels by summing over all lower-lying states and inverting.

III. COMPARISON OF ATOMIC SPIN–ORBIT CI RESULTS

The use of RECPs is bound up with several approximations beyond those generally associated with *ab initio* calculations. To test how the present treatment employing the RECP of Ross *et al.*³⁶ measures up we have carried out a series of calculations for the mercury atom and its positive ions for comparison with benchmark energy results recently reported by Häussermann *et al.*²⁴ These authors have compared various all-electron methods with pseudopotential treatments at both the Hartree–Fock and CI levels. Their RECP does not include the $5s$ and $5p$ subshells, unlike that of Ross *et al.* employed here, so one of the interesting aspects of this study is to assess this distinction. From the outset, however, it should be recognized that treating the $5s$ and $5p$ electrons explicitly in the calculations implies that extra basis functions must be included relative to a description in which only the $5d$ and $6s$ electrons are in the active space. Hence, the fact that Basis I derived from Ref. 36 is considerably smaller than either Basis II or III adapted from

TABLE II. SCF excitation and ionization energies (eV) of the Hg atom from the relativistic all-electron (AE, DF) and effective core potential (ECP) calculations with various basis sets.

		Häussermann <i>et al.</i> ^c				This work		
			AE, DF	ECP		Basis sets ^b		
	Configuration	LS	FDM ^a	FDM ^a	(II)	(I)	(II)	(III)
Hg	$5d^{10}6s^2$	1S	0	0	0	0	0	0
	$5d^{10}6s^16p^1$	3P	3.856	3.833	3.820	3.769	3.793	3.754
		1P		5.663	5.661	5.723	5.732	5.672
Hg ⁺	$5d^{10}6s^1$	2S	8.547	8.513	8.514	8.609	8.661	8.580
	$5d^96s^2$	2D	14.030	14.055	14.110	14.068	14.084	14.104
	$5d^{10} \quad 6p^1$	2P	15.230	15.174	15.163	15.362	15.433	15.321
	$5d^{10} \quad 6d^1$	2D		20.161	20.197	20.514	20.557	20.449
Hg ²⁺	$5d^{10}$	1S	25.692	25.624	25.617	25.876	25.999	25.808
	$5d^96s^1$	3D	31.616	31.699	31.738	31.603	31.652	31.608
		1D		32.712	32.750	32.864	32.918	32.859

^aResults obtained with a finite difference method (FDM).^bBasis sets: (I) (3s3p4d) basis set (Ref. 36) plus (1s1p1d). (II) {(8s8p7d)/[6s6p4d] plus (1s1p1d2f)} ECP basis set (Ref. 24). (III) (9s9p8d4f) uncontracted basis set [with the smallest exponents of the (21s19p16d9f) all-electron basis set (Ref. 24)] plus (1p).^cReference 24.

the work of Häussermann *et al.*²⁴ is to a large extent a reflection of the difference in the number of electrons to be treated in computations employing their respective RECPs.

Excitation and ionization energies calculated at the SCF level of treatment for the mercury atom are compared in Table II. All energy values are given relative to the respective ...5d¹⁰6s² Hg atom ground state result obtained within a given theoretical treatment. At the all-electron Dirac–Fock level the Hg ³P excitation energy is 3.856 eV.²⁴ When the RECP of Ref. 24 is employed and the resulting Schrödinger equation is solved numerically (finite difference method) a result of 3.833 eV is obtained, an error of only 0.023 eV compared to the DF treatment. Use of an expansion method with Basis II gives a result which is only 0.013 eV lower than the numerical value obtained with the same RECP. Switching to the Ross *et al.* RECP,³⁶ with the 5s,5p Hg electrons described by the core potential, produces somewhat lower values (by 0.03–0.08 eV) for this excitation energy, depending on which AO basis is employed. It should be noted that all of the present SCF results are obtained by completely neglecting the spin–orbit interaction, while the AE, DF values with which these results are compared are obtained by averaging individual multiplet energies belonging to the same Λ – S state.

Similar results are obtained for the ¹P excitation energy, although comparison with the all-electron DF result is not possible in this case.²⁴ It is found that an exponent near 0.012 a_0^{-2} is essential to obtain good results for this quantity. Substituting the Ross *et al.* RECP leads to an increase of 0.071 eV relative to the analogous treatment with the Häussermann *et al.* RECP²⁴ when Basis II continues to be employed.

Moving on to Hg⁺, it is seen that the DF ionization energy is 0.034 eV larger than that obtained with the RECP of Ref. 24 and numerical methods and 0.033 eV larger than

with Basis II. Use of the Ross *et al.* RECP³⁶ leads to uniformly higher values for this quantity, whereby the result with Basis I is only 0.062 eV larger than the DF value while that of Basis II is 0.114 eV higher. Dirac–Fock values for the 5d⁹6s² ²D and 5d¹⁰6p¹ ²P ionization energies are also available. In the case of the ²D ion there is a somewhat larger discrepancy between the numerical result and that found with Basis II in Ref. 24. Each of the three values in Table II obtained with the Ross *et al.* RECP³⁶ falls in between these two results. For Hg⁺ ²P the results obtained with the latter RECP overestimate the corresponding DF value by 0.1–0.2 eV, while the two results for the Häussermann *et al.* RECP fall below this value by 0.06–0.07 eV. There is no DF result for the 5d¹⁰6d¹ ²D Hg⁺ state.

Results for the Hg²⁺ ion may also be compared in Table II. The closed-shell ¹S ground state has an ionization energy of 25.692 eV at the all-electron DF level. Use of the RECP of Ref. 24 leads to somewhat lower results (errors of 0.068 and 0.075 eV, respectively, for the numerical and Basis II treatments). The corresponding energy values for the Ross *et al.* RECP³⁶ are all too high (0.1–0.3 eV) by contrast. The situation for the 5d⁹6s¹ ³D state is somewhat different, with all the results with the Ross *et al.* RECP³⁶ lying within 0.05 eV of the all-electron DF value, and those with the Häussermann *et al.* potential²⁴ lying too high by 0.08–0.12 eV. Finally, no comparable DF result for Hg²⁺ ¹D is available. Altogether it can be concluded that the relatively simple theoretical treatment based on the RECP and AO basis of Ref. 36 performs reasonably well at the Hartree–Fock level, with errors relative to exact all-electron Dirac–Fock values usually falling below 0.1 eV for this group of neutral and ionic states.

The next set of comparisons is carried out at the Λ – S CI level of treatment (Table III), again without consideration of the spin–orbit interaction. The importance of electron corre-

TABLE III. Excitation and ionization energies (eV) of Hg obtained in the effective core potential configuration interaction calculations without SO coupling in comparison to experimental data.

Häussermann <i>et al.</i> ^a							
Configuration	LS	CIPSI	CASSCF		This work Basis set (I)	Expt. ^b	
			+MRCI	ACPF			
Hg	$5d^{10}6s^2$	1S	0	0	0	0	
	$5d^{10}6s^16p^1$	3P	5.332	5.219	5.229	5.046	5.182
		1P	6.718	6.896	6.913	6.676	6.704
Hg ⁺	$5d^{10}6s^1$	2S	10.242	10.039	10.034	10.020	10.438
	$5d^96s^2$	2D	15.033	15.013	15.010	15.156	15.588
	$5d^{10}6p^1$	2P	17.529	17.243	17.239	16.992	17.576
Hg ²⁺	$5d^{10}$	1S	28.859	28.381	28.371	28.009	29.189
	$5d^96s^1$	3D		34.281	34.274	33.986	35.019
		1D		35.063	35.055	34.911	36.763

^aReference 24.^bReference 45.

lation effects can be judged by comparing the experimental excitation and ionization energies⁴⁵ in this table with the corresponding Dirac–Fock values already discussed (Table II). The Hg ³P excitation energy is 5.182 eV, for example, 1.326 eV higher than predicted at the DF level. The corresponding Hg⁺ IP is computed to be only 8.547 eV, a nearly 1.9 eV underestimation. For Hg²⁺ the DF errors climb to 3.0–3.5 eV compared to measurement. It should therefore be clear that in order to obtain the maximum in benefit from any relativistic treatment of such quantities, it is essential to describe electron correlation effects to a high degree of accuracy.

The results shown in Table III are spin averaged. Three different results from the work of Häussermann *et al.*²⁴ are shown in most cases, one employing the CIPSI⁴⁶ method, the other two based on an initial CASSCF treatment (MRCI and ACPF). In all these calculations the RECP of Ref. 24 has been employed, i.e., the 5s and 5p Hg electrons have been treated explicitly in the CI calculations. These results are compared with those obtained with Basis I and the RECP of Ross *et al.*³⁶ The latter calculations lead to an underestimation of the ³P excitation energy by 0.13 eV, while those of Ref. 24 overestimate this quantity by 0.04–0.15 eV. The present result for the ¹P excitation energy is only 0.028 eV in error. The CIPSI treatment is even more accurate in this case, whereas the two CASSCF values are too high by 0.2 eV.

The situation is less satisfactory for all the treatments when attention is directed toward Hg⁺. The present ground state ionization energy is underestimated by 0.418 eV, for example. The CIPSI calculated result corresponds to only about half as large an error, but the two CASSCF results are also too low by 0.4 eV. The ²D–²S Hg⁺ energy splitting (5.150 eV, obs.) comes out well in the present treatment (5.136 eV), however, which naturally means that the ²D ionization energy relative to the Hg ground state is also too low by 0.4 eV. In each of the three treatments of Ref. 24 this quantity is underestimated by 0.55–0.57 eV. The same level of accuracy is found in the present treatment for the 5d¹⁰6p¹ ionization energy (0.584 eV underestimation). In this case

the calculations of Ref. 24 are more accurate, especially the CIPSI value, which is only 0.047 eV too low. This good agreement may simply result from a cancellation of errors, however, because the MRCI and ACPF values based on CASSCF MOs are nearly 0.3 eV smaller.

The tendency to underestimate ionization energies in the present treatment based on the Ross *et al.* RECP³⁶ is strengthened for the mercury doubly positive ion. For the three states considered errors of 1.0–1.8 eV are noted in these calculations, whereas somewhat smaller discrepancies are found whenever the Häussermann *et al.* RECP²⁴ is employed in the CASSCF+MRCI/ACPF treatments (0.8–1.7 eV errors). Again the CIPSI value for the Hg²⁺ ¹S ionization energy is notably more accurate than any of the other results, indicating more than likely that the CI error in this case is significantly larger for the ion than for the ¹S neutral ground state. The overall conclusion from the spin-averaged (Λ–S) CI results is that the excitation energies between atomic states with the same number of electrons can be predicted with considerably higher accuracy when either of the two RECPs^{24,36} is employed than can ionization energies relative to the same electronic states.

The final comparison of the present results with experimental values and those of earlier theoretical work is for the excitation energies of the Hg atom and its ions after the execution of the spin–orbit CI treatment (Table IV). In this case only the CIPSO results of Ref. 24 are available. The Hg ³P state splits into three term levels, in the energetic order *J*=0<1<2. The CIPSO values are in generally better agreement with the observed data than are those obtained in the present treatment. The spin–orbit part of the RECP of Ref. 24 seems to be mainly responsible for the better agreement of the CIPSO ³P results. Häussermann *et al.*²⁴ point out that the parameters for their spin–orbit operator have been adjusted to reproduce splittings corresponding to a large number of configurations which result from multiconfigurational Dirac–Fock (MCDF) calculations,⁴⁷ these in turn being in quite good agreement with the corresponding measured data. Based on the present results for multiplet splittings it would

TABLE IV. Excitation energies (cm⁻¹) of the lowest-lying states of Hg, Hg⁺, and Hg²⁺ obtained in the ECP calculations with SO coupling in comparison with experimental data.^a

	Configuration	LS	<i>J</i>	CIPSO ^b	This work Basis set (I)	Expt. ^c
Hg	5d ¹⁰ 6s ²	¹ S	0	0	0	0
	5d ¹⁰ 6s16p ¹	³ P	0	37 738	37 193	37 645
Hg ⁺	5d ¹⁰ 6s ¹	² S	1/2	0	0	0
	5d ⁹ 6s ²	² D	5/2	34 350	35 932	35 514
			3/2	48 782	49 566	50 552
Hg ²⁺	5d ¹⁰ 6p ¹	² P	1/2	52 564	50 614	51 485
			3/2	60 860	58 948	60 608
	5d ¹⁰	¹ S	0	0	0	0
Hg ²⁺	5d ⁹ 6s ¹	³ D	3	41 664	42 734	42 850
			2	44 818	46 567	46 030
			1	56 459	56 868	58 406
		¹ D	2	59 610	60 395	61 086

^aIonization potentials remain unchanged; see Table III.

^bReference 24.

^cReference 45.

appear that the spin-orbit operator in the Ross *et al.* RECP³⁶ should itself be adjusted to give a more accurate energy separation between the ³P *J*=0, 1, and 2 states.

Especially when the results for the ¹P state are taken into account, however, it seems fair to conclude that the results obtained with the Ross *et al.* RECP³⁶ are still quite acceptable. This view is reinforced when attention is turned to the corresponding data for Hg⁺ and Hg²⁺ (Table IV). In this case the excitation energies relative to the respective ²S and ¹S ground states are computed with even somewhat higher accuracy in the present treatment than with the CIPSO calculations based on the Häussermann *et al.* RECP.²⁴ For example, the Hg⁺ ²D_{5/2} excitation energy is overestimated by 418 cm⁻¹ in the present calculations, while it is underestimated by 1164 cm⁻¹ in the CIPSO treatment.²⁴ The two theoretical results for the ²P_{1/2} excitation energy are of about equal accuracy, albeit with errors in opposite directions. Finally, the CIPSO result is notably more accurate for the ²P_{3/2} excitation energy than is the present value, but the error in the latter case is still only about 0.2 eV. Again the ²P spin-orbit splitting is computed to be too small in the present calculations with the Ross *et al.* RECP (8334 cm⁻¹ vs 9123 cm⁻¹), but in this case it is very nearly the same as obtained with the CIPSO method.²⁴ Very similar conclusions result from an analysis of the corresponding Hg²⁺ excitation energies. Of particular interest is the result that the ¹D₂-¹S₀ excitation energy is only 691 cm⁻¹ in error (Table IV) in the treatment with spin-orbit coupling even though the corresponding averaged ¹D-¹S Λ-S value differs by 5420 cm⁻¹ (Table III) from the corresponding result deduced from experimental data. This result emphasizes that it is dangerous to judge the level of accuracy of calculations for such heavy systems without giving careful consideration to the effects of spin-orbit coupling. Finally, it can be noted that although the CIPSO results²⁴ have a definite advantage with regard to the

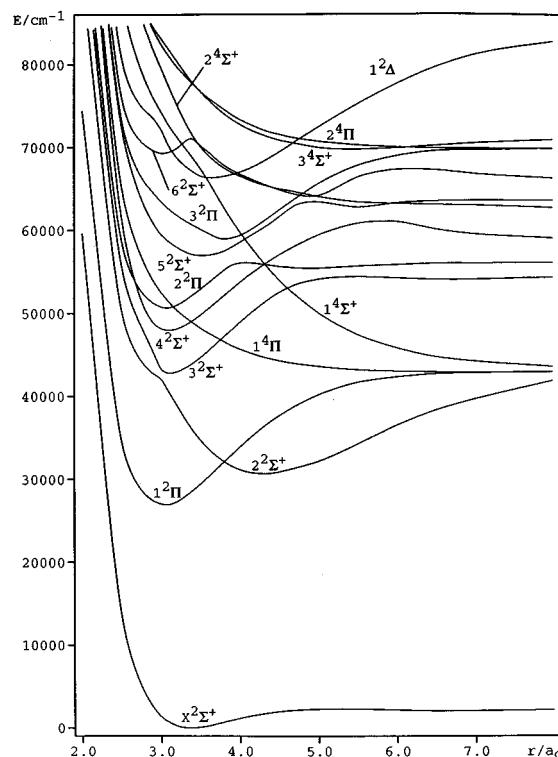


FIG. 1. Computed potential energy curves for the lowest-lying Λ-S states of the HgH molecule obtained in a theoretical treatment without the inclusion of the spin-orbit interaction.

size of spin-orbit multiplet splittings within a given Λ-S state, on an absolute basis the computed Hg²⁺ excitation energies of the present treatment are still found to be more accurate in every case.

IV. POTENTIAL ENERGY CURVES FOR HgH

The calculated CI potential curves for the lowest-lying Λ-S states of HgH up to 80 000 cm⁻¹ are shown in Fig. 1. The ground state is the weakly bound X ²Σ⁺ with a σ²σ* electronic configuration. The excited states are generally formed by occupying either the π* MO or Rydberg orbitals of 7s and 7p type. Configurations with open Hg 5d shells are relatively unimportant in the excitation process for the HgH CI calculations, and thus the lack of *f*-type polarization functions in the AO basis (see Sec. II) should not seriously affect the reliability of the present theoretical treatment. The lowest dissociation limit is Hg 6s²(¹S_g)+H(²S_g), and it correlates only with the molecular ground state. Its potential curve has a slight maximum corresponding to a strongly avoided crossing with the 2²Σ⁺ state, or more precisely, to an abrupt change from the repulsive character of pure 6s_{Hg}σ and 1s_Hσ* orbitals near the dissociation limit to Hg-H σ and σ* bonding and nonbonding orbitals at short distances (see discussion in Ref. 21). The first excited state (A ²Π) arises from a σ*→π* excitation and has a much deeper potential well than the ground state. It dissociates to the ³P_u excited state of the Hg atom, along with the 2²Σ⁺ and the lowest ⁴Π and ⁴Σ⁺ states (Fig. 1). The A ²Π and 2²Σ⁺ potential curves cross near *r*=4.0 *a*₀, the latter arising from a

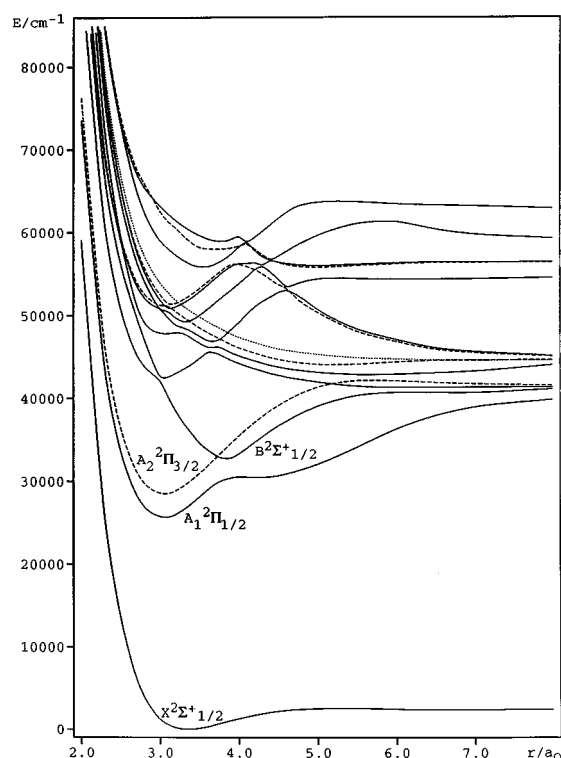


FIG. 2. Computed potential energy curves for the low-lying states of the HgH molecule (solid lines: $\Omega=1/2$, dashed lines: $\Omega=3/2$, dotted line: $\Omega=5/2$).

$\sigma \rightarrow \sigma^*$ excitation. The two quartet states have leading contributions from the $\sigma \rightarrow \pi^*(6p), 7s, 7p$ excitations and are repulsive in character.

There is a sharply avoided crossing between the $2^2\Sigma^+$ and $3^2\Sigma^+$ states which produces a fairly deep well in the upper of these two states. At distances near the r_e value for the ground state the $3^2\Sigma^+$ is primarily a $\sigma \rightarrow 7s$ Rydberg species, but it dissociates to the $6s6p\ ^1P_u$ state along with $2^2\Pi$. The latter has an avoided crossing with $3^2\Pi$ near $r=4.0\ a_0$. The $4^2\Sigma^+$ state, which arises from a $\sigma \rightarrow 7p$ excitation, lies below the $2^2\Pi$ state at small r values (Fig. 1). It is the first state to dissociate to the Hg $6s7s\ ^3S_g$ Rydberg state, and it possesses a deep potential minimum as well as a maximum in energy near $r=6.0\ a_0$. The $5^2\Sigma^+$ state lies between $2^2\Pi$ and $3^2\Pi$ and also has a deep potential well. At still higher energies the density of states becomes fairly high in the $X^2\Sigma^+$ Franck–Condon region.

After adding spin–orbit coupling to the theoretical treatment the potential curves of Fig. 2 result. The composition of the final spin-perturbed states in terms of Λ – S eigenfunctions is sketched in Tables V ($\Omega=1/2$) and VI ($\Omega=3/2$). The ground state is almost exclusively $X^2\Sigma^+$, especially at large r values. Spectroscopic constants for a number of the low-lying HgH states are given in Table VII. Four different experimental r_e values for the ground state have been reported,^{1,12,15,48} ranging from 1.735 to 1.766 Å. The largest of these values is preferred by Huber and Herzberg⁴⁸ and it is in good agreement with the present computed result of 1.777

Å. Other calculated results fall between 1.725 and 1.795 Å. The smallest of these was obtained by Bernier *et al.*,²² 0.052 Å less than our result. The corresponding value computed in Ref. 24, whose Hg atom calculations have been considered in the previous section, is 1.795 Å.

The situation is even less clear for the experimental ω_e value, originally cited by Herzberg¹⁵ as 1387 cm^{−1} but given in parentheses with the remark “effective constants” as only 1203 cm^{−1} in Ref. 48. Häussermann *et al.*²⁴ have calculated a value of 1160 cm^{−1}. Bernier *et al.*²² have found nearly the same result as in the present work, while that of Hay *et al.*²¹ is 86 cm^{−1} smaller. We find a potential maximum near $r=5.0\ a_0$, which is consistent with remarks made earlier by Mulliken¹⁴ and Hay *et al.*²¹ Stwalley¹ was able to fix the D_0^0 value of $X^2\Sigma^+_{1/2}$ at 0.3744 eV or 3020 cm^{−1}, which corresponds to a D_e of 3700 cm^{−1}.¹² The present calculated result is only 2543 cm^{−1}, whereas the CIPSO of Ref. 24 is 3847 cm^{−1}.

The $A^2\Pi$ state is split regularly by the spin–orbit interaction. The lower-lying $A_1^2\Pi_{1/2}$ undergoes an avoided crossing with $B^2\Sigma^+_{1/2}$ near $r=3.9\ a_0$ (Fig. 2 and Table V). At still larger r values the 4Π and $4\Sigma^+$ Λ – S states also make important contributions to A_1 . It dissociates to the $3P_0$ state of the mercury atom. By contrast the $A_2^2\Pi_{3/2}$ component is much less perturbed in the Franck–Condon region of $X^2\Sigma^+_{1/2}$. It has a large admixture of 4Π and $4\Sigma^+$ character (Table VI) beyond $r=5.0\ a_0$, however. The present computed T_e value of the $A_1^2\Pi_{1/2}$ state is about 1000 cm^{−1} higher than observed.^{11,12,15} Several earlier theoretical values^{21,22,24} are in better agreement with experiment, with each of them also being an overestimate [from 150 cm^{−1} (Ref. 22) to 470 cm^{−1} (Ref. 21)]. The present result for the $A_2^2\Pi_{3/2}$ T_e value is only 200 cm^{−1} too high,^{15,48} however, and as such is in better agreement with the observed value than in previous theoretical work. The A_1 – A_2 energy splitting is given quite well by the calculations of Häussermann *et al.*,²⁴ which again underscores the superiority of their RECP in this regard. In the present treatment this splitting is 2826 cm^{−1}, compared to 3678 cm^{−1} observed,¹⁵ an underestimation which is consistent with experience with the atomic calculations of Sec. III.

The bond lengths of both the A_1 and A_2 states are calculated to be 1.615 Å, so about 0.03 Å too large in each case. Our results agree to within 0.01 Å of those given in Ref. 24 and also mesh quite well with those of Bernier *et al.*²² The best agreement with the observed r_e values is obtained by Hay *et al.*,²¹ however, but their corresponding ω_e values are 400 cm^{−1} too small in each case. The present computed frequencies are too low by 43 and 36 cm^{−1}, respectively.

The $B^2\Sigma^+_{1/2}$ state is the highest-energy HgH species for which detailed spectroscopic information is yet available. Its experimental bond length has been reported to lie between $r=2.030$ ¹⁵ and 2.080 Å,¹³ whereas Huber and Herzberg⁴⁸ favor a value of 2.043 Å. Because the minimum of this state arises from a strongly avoided crossing with $A_1^2\Pi_{1/2}$ (Fig. 2), it is perhaps not surprising that there should be such uncertainty in the corresponding r_e value. The present calculations obtain $r=2.026\ Å$, while earlier theoretical

TABLE V. Composition of the nine lowest $\Omega=1/2$ states of HgH [c^2 (%)] at various bond distances r .

State	r/a_0	$1^2\Sigma^+$	$2^2\Sigma^+$	$3^2\Sigma^+$	$4^2\Sigma^+$	$5^2\Sigma^+$	$1^2\Pi$	$2^2\Pi$	$3^2\Pi$	$4^2\Pi$	$5^2\Pi$	$1^4\Pi^a$	$1^4\Sigma^+$
$X_1^2\Sigma_{1/2}^+$	2.8	98.7											
	3.3 ^b	99.3											
	5.0	99.9											
	8.0	100.0											
	18.0	100.0											
$A_1^2\Pi_{1/2}$	2.8	1.0					98.6						
	3.05 ^b						98.9						
	3.85		35.1				64.2						
	4.0		73.5				25.6						
	5.0		95.8				2.8					1.0	
	8.0		23.2				23.6					39.3	13.5
	18.0		10.0				20.8					46.5	22.4
	2.8		97.8										
	3.05		78.1	17.0								2.5	
	3.5		95.3				1.8					1.6	
$B^2\Sigma_{1/2}^+$	3.85 ^b		63.3				35.1						
	4.0		25.1				73.7						
	5.0		2.4				92.7					3.4	
	8.0		34.0				1.0					46.3	17.4
	18.0		14.6				1.9					71.6	7.5
	2.8			82.2	9.4							5.0	
	3.05 ^b		20.9	74.5								2.4	
	3.5			96.9								2.4	
	3.65		1.0	26.7								70.5	
	4.0											97.7	
$1/2(IV)$	8.0		1.4				40.3					56.4	
	18.0		16.0				50.3					24.5	6.8
	2.8			15.7	70.2							11.0	
	3.2		1.3	1.0	72.6							23.2	
	3.5		1.1	2.1	1.2							94.0	
	3.65			61.4								37.8	
	4.0											97.1	
	5.0		1.2				3.1					93.0	1.8
	8.0		40.8				33.5					24.6	
	18.0		6.0				4.2					39.8	49.4
$1/2(VI)$	2.8							98.6					
	3.0							81.3				17.3	
	3.3				32.1							65.3	
	3.5			1.0	2.1							93.5	
	3.65 ^b			11.9								84.9	
	4.0			99.6									
	5.0							1.0				7.1	91.4
	8.0											32.0	67.5
	18.0		51.4				24.7					12.1	11.7
	2.8				3.1							94.1	
$1/2(VII)$	3.0				2.9			13.5				80.6	
	3.3 ^b				47.8			1.8				48.1	
	4.0				98.7								
	4.25				91.6			5.6					1.4
	4.6							4.8				4.4	90.3
	5.0			98.9									
	8.0			95.5			1.1	3.2					
	18.0			4.1				94.5					
	2.8			1.0	13.9	1.3						80.9	
	3.15 ^b				2.7			87.8				8.5	
$1/2(VIII)$	3.5							98.7					
	4.0					2.7		95.1					
	4.25				7.2			65.5				1.7	24.8
	4.4				57.0			31.0					11.1
	5.0							97.6					1.4
	8.0				3.3			95.3					
	18.0			94.5				4.1					
	2.8					91.3				2.5	2.9	2.0	
	3.0					89.8				3.0	1.2	1.8	
	3.5 ^b					85.3				11.8			

TABLE V. (Continued.)

State	r/a_0	$1^2\Sigma^+$	$2^2\Sigma^+$	$3^2\Sigma^+$	$4^2\Sigma^+$	$5^2\Sigma^+$	$1^2\Pi$	$2^2\Pi$	$3^2\Pi$	$4^2\Pi$	$5^2\Pi$	$1^4\Pi^a$	$1^4\Sigma^+$
	4.1					52.7			11.7				30.2
	4.4				41.9			46.7					10.8
	5.0				99.2								
	8.0				99.2								
	18.0												100.0

^aSince the 4Π Λ - S state contains two distinct $\Omega=1/2$ components, each normalized to unity, the sum of c^2 contributions in this column for a given bond distance has a theoretical maximum of 200%.

^bApproximate r_e value.

predictions^{21,22,24} lie in the 2.07–2.08 Å range. The corresponding observed ω_e value is 2004 cm⁻¹,¹³ whereas the present computed result lies 152 cm⁻¹ higher. The corresponding result of Häussermann *et al.*²⁴ is much higher (2901 cm⁻¹), however, while that of Ref. 22 appears to be too low by nearly 400 cm⁻¹. The present T_e value for $B^2\Sigma^+_{1/2}$ is less than 200 cm⁻¹ lower than the observed value, which again is quite acceptable agreement for this level of theoretical treatment.

Two other $2\Sigma^+$ states have been inferred from spectroscopic data^{4,8,16} assigned as $C-X$ and $D-X$ transitions. There is some question about the interpretation of these experimental results, however, because it attributes ν_{00} values of 35 587.4 and 37 040 cm⁻¹ to the assumed transitions, which seem too low to be consistent with theoretical find-

ings. For example, the lowest $\Omega=1/2$ states above $B^2\Sigma^+$ are computed in the present study to have values of 42 509 and ~47 900 cm⁻¹, respectively (Table VII). Furthermore, the calculated r_e value for 1/2 (IV) is 1.628 Å, which is 0.3 Å less than the suggested experimental bond length for the C upper state. The latter computed state arises from a strongly avoided curve crossing as well, and there is some question whether suitably stable vibrational states could result from the corresponding potential well. The results of Table V show that the 1/2 (IV) state starts out as $\sigma^* \rightarrow 7s$ before changing to $4\Pi_{1/2}$ (see also Fig. 2). The four 4Π Ω multiplets are all nearly repulsive, with no potential minima for $r < 3.0$ Å. Huber and Herzberg⁴⁸ characterize the $C-X$ and $D-X$ spectra as only fragmentary and so it seems best to look for another interpretation for these observations than that first suggested. Such an explanation was proposed, for example, by Nedelec *et al.*¹³ who have assigned the two observed bands in question to the $v'=1$ and 2 vibrational levels of the $B^2\Sigma^+$ state, and the present computed spectroscopic constants are found to be in good agreement with those inferred experimentally on the basis of this assignment.

The accuracy of the present CI calculations, independent of the choice of AO basis and RECP, seems to be relatively high based on analysis of energy results for different states of the separated atoms. At the full CI level one knows that the energies of all molecular states for very large r values corresponding to a particular atomic limit must be equal to the corresponding sums of atomic energies obtained with the same AO basis (and RECP). The computed $3P_0-1S$ excitation energy in the present treatment is 37 280 cm⁻¹ in the molecular treatment ($A_1^2\Pi_{1/2}-X^2\Sigma^+_{1/2}$) and 37 193 cm⁻¹ for the mercury atom alone. For $3P_1$ the atomic T_e value is 38 722 cm⁻¹ only 40 cm⁻¹ different than the average excitation energy at large bond lengths (38 712 cm⁻¹ for three states). There are five molecular states which correlate with $Hg(^3P_2)+H(^2S_{1/2})$ and their computed average excitation energy is 42 175 cm⁻¹ at large r , compared to the corresponding atomic value of 42 416 cm⁻¹. Finally, the analogous comparison for the $1P_1$ asymptote is 53 973 cm⁻¹ (molecular) and 54 039 cm⁻¹ (atomic). Such agreement between CI energies of large- r molecular and corresponding atomic states is typical for MRD-CI calculations employing the perturbative corrections mentioned in Sec. II, as, for example, has recently been demonstrated for the HeN⁺ molecular ion.⁴⁹ In other words, when discrepancies in such calculated quantities and their confirmed experimental values exceed

TABLE VI. Composition of the four lowest $\Omega=3/2$ states of HgH [c^2 (%)] at various bond distances r .

State	r/a_0	$1^2\Pi$	$2^2\Pi$	$3^2\Pi$	$4^2\Pi$	$5^2\Pi$	$1^4\Pi$	$1^4\Sigma^+$	$1^2\Delta$
$A_2^2\Pi_{3/2}$	2.8	99.6							
	3.05 ^a	99.6							
	4.0	99.6							
	5.0	90.1					7.5	1.9	
	6.0	36.4	1.1				45.7	16.6	
	8.0	19.0	1.1				39.1	40.5	
	18.0	15.2	1.4				35.8	44.5	
3/2(II)	2.8		99.8						
	3.15		10.6				86.1		
	4.0						97.4		
	5.0	9.1					86.1	3.6	
	6.0	59.3					39.8		
	8.0	59.9					38.7		
	18.0	34.1					56.4	8.8	
3/2(III)	2.8						95.2		
	3.15 ^a		89.3				10.2		
	3.5		99.3						
	4.0		93.5	1.2				3.7	
	5.0		3.8				5.8	89.4	
	8.0	20.4					21.4	58.0	
	18.0	47.5					9.1	42.1	
3/2(IV)	2.8			94.4					1.0
	3.0			22.4	57.1	3.3			6.9
	3.75 ^a			53.5		35.5		2.0	7.0
	4.0		1.5	38.6		34.6		14.3	8.9
	4.1		8.7	22.4		15.9		47.4	4.2
	5.0		94.6					4.7	
	8.0		98.5						
	18.0		98.5						

^aApproximate r_e value.

TABLE VII. Calculated and experimental spectroscopic properties of HgH (transition energies T_e , bond lengths r_e , and vibrational frequencies ω_e).^a

State	$T_e(\text{cm}^{-1})$		$r_e(\text{\AA})$		$\omega_e(\text{cm}^{-1})$	
	Calc. [Ref.]	Expt. [Ref.]	Calc. [Ref.]	Expt. [Ref.]	Calc. [Ref.]	Expt. [Ref.]
$X\ ^2\Sigma^+_{1/2}$	0	0	1.777 1.783 [20] 1.763 [21] 1.725 [22] 1.795 [24]	1.735 [1] 1.741 [12] 1.740 [15] 1.766 [48]	1309 1123 [20] 1227 [21]	1387 [4,7] 1385 [12] 1203 [48]
$A_1\ ^2\Pi_{1/2}$	25 664 29 117 [20] 25 084 [21] 24 761 [22] 25 008 [24]	24 609 [11] 24 590 [12] 24 578 [15]	1.615 1.593 [20] ^b 1.579 [21] 1.619 [22] 1.603 [24]	1.583 [11] 1.583 [12] 1.586 [15] 1.601 [48]	2023 2032 [20] ^b 1629 [21] 1969 [22] 1948 [24]	2031 [11] 2068 [12] 2066 [15] 1939 [48]
$A_2\ ^2\Pi_{3/2}$	28 490 32 423 [20] 28 068 [21] 27 794 [22] 28 719 [24]	28 283 [12] 28 256 [15] 28 274 [48]	1.615 1.575 [21] 1.622 [22] 1.610 [24]	1.581 [12] 1.580 [15] 1.579 [48]	2033 1686 [21] 1865 [22] 1930 [24]	2091 [12] 2067 [15] 2068 [48]
$B^2\ ^2\Sigma^+_{1/2}$	32 723 31 778 [21] 31 520 [22] 31 945 [24]	32 909 [13]	2.026 2.078 [21] 2.079 [22] 2.068 [24]	2.080 [13] 2.030 [15] 2.043 [48]	2156 1604 [21] 1639 [22] 2901 [24]	2004 [13]
1/2(IV)	42 509		1.628		3036	
1/2(V)	~47 900					
1/2(VI)	46 820		1.934		2718	
1/2(VII)	49 271		1.757		2575	
1/2(VIII)	50 977		1.671		2557	
3/2(III)	51 444		1.679		2564	
1/2(IX)	55 840		1.882		1705	

^aEntries without references are results of the present work.^bObtained for both $A\ ^2\Pi$ components.

200 cm⁻¹, the indication is that sources of error (AO basis and RECP) other than the CI treatment itself must be involved.

V. LIFETIMES OF HgH STATES

The spin-orbit CI wave functions for the HgH molecule discussed in the last section have been employed to compute transition probabilities between pairs of vibrational states. The results of these calculations for different transitions to the $X\ ^2\Sigma^+_{1/2}$ ground state in the form of $v'=0$ radiative lifetimes are contained in Table VIII. There have been three detailed experimental studies of the lifetime of the $A_1\ ^2\Pi_{1/2}$ excited state^{10–12} and their results are in very close agreement with one another. Dufayard *et al.*¹² have also measured the lifetime of the $A_2\ ^2\Pi_{3/2}$ state. In the case of the A_1 state there is competition between radiative and nonradiative processes, the latter caused by an interaction with the inner limb of the $X\ ^2\Sigma^+_{1/2}$ potential curve (see Fig. 2). Clear evidence for this comes from the fact that the lifetime of the $v'=0$ HgH A_1 level is measured to be 100–101 ns^{10–12} whereas that of the heavier deuteride isotopomer is significantly longer (131–133 ns). It has been estimated on this basis (assuming that there is no predissociation in HgD, $v'=0$ and that the dipole transition moment does not vary with internuclear distance) that the true radiative lifetime in HgH, $v'=0$, is 132 ± 4 ns.¹²

The computation of the required transition probabilities depends to a significant degree on the accuracy of the relevant potential curves. The present CI results for both the $A\ ^2\Pi$ and $X\ ^2\Sigma^+$ states have been found to have some deficiencies, especially with respect to the well depth of the

TABLE VIII. Radiative lifetimes (ns) of excited states of HgH ($v'=0$) for transitions to the $X\ ^2\Sigma^+$ ground state: calculated partial lifetimes τ_{\perp} and τ_{\parallel} for perpendicular and parallel contributions, respectively, as well as calculated and experimental total lifetime τ .

State	Calculated			Experimental
	τ_{\perp}	τ_{\parallel}	τ	
$A_1\ ^2\Pi_{1/2}$	95.0	22 200	94.6	$134\pm 3^{\text{a,b}}$ $131^{\text{a,c}}$ $132\pm 4^{\text{d}}$ $91\pm 3^{\text{d}}$
$A_2\ ^2\Pi_{3/2}$	64.2		64.2	
$B^2\ ^2\Sigma^+_{1/2}$	167	56.6	42.3	
1/2(IV)	972	7.6	7.5	
1/2(VI)	910	18.6	18.2	
1/2(VII)	910	25.3	24.7	
1/2(VIII)	3327	640	537	
1/2(IX)	1950	1.5	1.5	
3/2(III)	1990		1990	

^aMeasured for the HgD molecule; see text.^bReference 10.^cReference 11.^dReference 12.

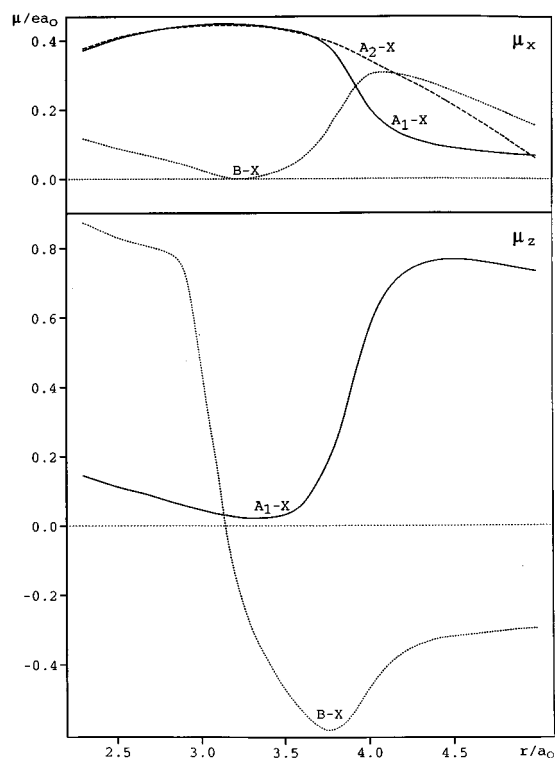


FIG. 3. Computed electric dipole transition moments μ_x (upper part) and μ_z (lower part) between various electronic states of the HgH molecule as a function of internuclear distance r . The molecule is located on the z axis.

ground state. Fortunately RKR curves which are based on empirical data are available for each of the interesting states. The present calculated $X\ ^2\Sigma_{1/2}^+$ potential minimum occurs at nearly the same r value as its RKR counterpart, so the main distinctions between them appear at somewhat larger bond distances. The $A_1\ ^2\Pi_{1/2}$ RKR curve lies somewhat lower than the calculated one (Table VII), but it is unsatisfactory at large r values. Because of the avoided crossing between the $B\ ^2\Sigma_{1/2}^+$ and A_1 states near $r=4.0\ a_0$, there is a shoulder in the lower potential curve which extends to beyond $r=4.5\ a_0$. This feature is totally missing in the A_1 RKR curve, but is not expected to play a significant role in the description of the lowest three vibrational levels of this state.

The present computed transition moments are shown in Fig. 3, and these have been employed in conjunction with the above RKR curves to calculate the desired transition probabilities and radiative lifetimes. The μ_x component is equal by symmetry to μ_y , and together they dominate in the A_1 - X system in the Franck-Condon region of the ground state since a $^2\Pi-^2\Sigma^+\ \Lambda-S$ (perpendicular) transition is mainly involved (see Tables V and VIII). Not surprisingly the A_2 - X transition moment is nearly identical for this range of bond distance (Fig. 3, upper part). Beyond $r=3.7\ a_0$, however, the $2\ ^2\Sigma^+$ state makes a large contribution to A_1 (Table V) but not to A_2 , and so the two μ_x curves become different at this point. At the same time, the μ_z component (Fig. 3, lower part) of the A_1 - X transition moment takes on increasing importance and actually dominates over the perpendicular

values at $r=4.0\ a_0$ and still larger distances. The B - $X\ \mu_z$ value passes through zero at $r=3.3\ a_0$, but is otherwise fairly large at all bond distances.

Near the $X\ ^2\Sigma_{1/2}^+\ r_e$ value, however, the $^2\Pi-^2\Sigma^+\ \mu_{x,y}$ perpendicular moment dominates for both the A_1 - X and A_2 - X transitions. The radiative lifetime for A_1 - X is thereupon computed to be 94.6 ns for the $v'=0$ level (Table VIII). This result is 40% shorter than that deduced from experiment for the true radiative lifetime (132 ± 4 ns), and hence within the range of error expected for calculations at the present level of treatment. Since the experimental RKR curves for the A_1 and X electronic states are assumed to be reasonably accurate, this means that the calculated transition moments, especially the $\mu_{x,y}$ components in the FC region, are most probably too large by about 20% on the average. The higher v' radiative lifetime values are computed to be progressively longer than that of $v'=0$, but this is likely caused by the fact that the effect of the ground state continuum levels has been neglected. The computed HgD lifetime is 94.3 ns, only 0.3 ns shorter than for HgH, emphasizing again that the observed difference in these two quantities (~ 30 ns) arises solely because of distinctions in the effectiveness of the predissociation mechanism for the two isotopomers. It would be interesting to compute the nonradiative transition probabilities as well in order to have a more definite assessment of this point, as in an earlier calculation for HeH,⁵⁰ but this has not been done in the present study.

Confirmation of the above interpretation comes from analogous calculations of the $A_2\ ^2\Pi_{3/2}\ v'=0$ radiative lifetime. It is computed to be 64.2 ns (Table VIII), compared with the observed value of 91 ± 3 ns, which corresponds again to a 40% underestimation. If one assumes that the A_1 - X and A_2 - X transition moments are exactly equal, one would expect the ratio of the observed $v'=0$ radiative lifetimes/Einstein coefficients of spontaneous emission (1.451) to be roughly the same as that of the inverse cube of the ratio of their respective ν_{00} values. Since the latter value is 1.499 based on the experimental data, one sees that such an assumption is valid to a relatively high degree of accuracy. The present calculated ratio of the same two lifetimes is 1.473, in very good agreement with that measured. It therefore appears that, except for a tendency to overestimate the relevant transition moments by about 20% each, the present treatment of the HgH electronic structure is capable of giving a quite reliable description of these radiative processes.

There are apparently no experimental data for the transition probabilities of the B - X system. The present calculated value for the $v'=0$ lifetime of the B state is 42.3 ns, about 30% shorter than computed for $A_2\ ^2\Pi_{3/2}$. Results for five other higher-lying $\Omega=1/2$ states ($v'=0$) are also given in Table VIII, as well as for the $3/2$ (III) state (see Table VII for spectroscopic constants of these states). In four of these cases the corresponding lifetimes fall in the 1–20 ns range. The high density of states in this region of the HgH spectrum makes it difficult to carry out quantitative experimental studies of the transition probabilities of these states and competing nonradiative processes must also be expected in each case.

VI. CONCLUSION

A spin-orbit CI technique has been employed in conjunction with relativistic core potentials (RECPs) to study the electronic structure of the mercury hydride molecule as well as of the mercury atom and its positive ions. It is found that the Ross *et al.* RECP³⁶ performs quite well, even though it includes all but the $5d$ and $6s$ Hg electrons in the core potential. Comparisons with the all-electron Dirac-Fock (AE, DF) calculations of Häussermann *et al.*²⁴ for Hg, Hg⁺, and Hg²⁺ demonstrate that the relatively small AO basis recommended for use with the RECP of Ref. 36 is capable of providing an accuracy of 0.2 eV for excitation energies up to 32 eV at the single-configuration level of treatment. In this respect it should be recalled that by eliminating all the inner core orbitals from the explicit calculations with the SCF and CI approaches, a considerably smaller range of basis functions is required than would otherwise be the case.

Correlation effects are seen to be of major importance in such calculations, however. The (AE, DF) treatment is in error relative to experiment by 1.326 eV for the $^3P_u-^1S_g$ excitation energy of the Hg atom and by 1.891 eV for its lowest ionization potential (spin-averaged results in each case). By contrast, the present 12-electron $\Lambda-S$ CI treatment is in error by 0.136 and 0.418 eV, respectively. Similar accuracy is obtained by Häussermann *et al.*²⁴ with their 20-electron CASSCF/MR-CI treatment (errors of 0.037 and 0.399 eV in this case). Furthermore, while it is obvious that the relegation of fewer electrons to the core potential and the use of substantially larger basis sets might well lead to increased accuracy, particularly when the level of excitation increases, it must also be recognized that such developments seriously compound the difficulties in achieving a suitably reliable description of correlation effects in the overall computations. The spin-orbit operator of Häussermann *et al.*²⁴ is seen to produce more accurate multiplet splittings within a given $\Lambda-S$ state than that of Ross *et al.*³⁶ employed in the present MRD-CI calculations. Still the present treatment gives better results for the $^1P_1-^1S_0$ excitation energy and also for most of the corresponding Hg⁺ and Hg²⁺ term values than the CIPSO treatment of Häussermann *et al.*,²⁴ and its overall errors relative to experiment are everywhere less than 0.2 eV for atomic and ionic excitation energies up to 8 eV (Table IV).

Extension of the present spin-orbit CI treatment with the $5d^{10}6s^2$ Ross *et al.*³⁶ RECP and AO basis augmented with diffuse s and p functions to the calculations of HgH molecular potential curves and transition probabilities is also found to produce quite useful accuracy for the successful interpretation of spectroscopic data for this system. Experimental results have been reported for the lowest four electronic states, but there is still considerable disagreement about the values of a number of the corresponding spectroscopic constants. The present treatment leads to bond lengths which are too large by 0.03–0.04 Å and ω_e values which are too low by 40–80 cm^{−1} for the $X\ ^2\Sigma_{1/2}^+$, $A_1\ ^2\Pi_{1/2}$, and $A_2\ ^2\Pi_{3/2}$ states. Such discrepancies may be partially caused by the fact that f -type functions which might improve the description of

d -electron correlation are absent in the AO basis. Such an effect has been found in the AgH/AuH study of McLean,⁵¹ for example. The RECP employed may have an influence on such results as well, especially since the $5s$ and $5p$ shells have been included in the core. It is worth noting, however, that both these factors have been explored in the theoretical treatment of Häussermann *et al.*,²⁴ but their calculated bond lengths and frequencies show similar trends as in the present work. The error is larger for the $B\ ^2\Sigma_{1/2}^+$ state's ω_e value but this is understandable because the corresponding potential minimum is found to arise from a relatively strongly avoided crossing with the lower $A_1\ ^2\Pi_{1/2}$ state. The computed T_e value is within 1100 cm^{−1} of the observed result for the A_1 state, while errors of only 200 cm^{−1} each are noted for the corresponding A_2 and B values.

The spin-orbit CI wave functions have also been employed to compute transition probabilities between the A_1 , A_2 , and X states. The $^2\Pi-^2\Sigma^+$ transition moment ($\mu_{x,y}$) dominates in both the A_1-X and A_2-X radiative processes in the Franck-Condon region of the ground state, but a μ_z component becomes important at large r values because of the admixture of $2\ ^2\Sigma^+$ in the A_1 upper state at these bond distances. In agreement with the experimental interpretation,^{10–13} it is concluded that there is competition between the radiative and predissociative mechanisms in the decay of the $A_1\ ^2\Pi_{1/2}$ state. The computed radiative lifetime of 94.6 ns is 40% smaller than that estimated from an analysis of the experimental data for both HgH and HgD (132 ± 4 ns). The same level of accuracy is found in calculations of the A_2 radiative lifetime (64.2 ns vs 91 ± 3 ns¹²), suggesting that the corresponding transition moments to the $X\ ^2\Sigma_{1/2}^+$ ground state are too large by about 20% each in the present theoretical treatment. The lifetime of the $B\ ^2\Sigma_{1/2}^+$ state is computed to be 42.3 ns, but there is no experimental result available in this case. The present study agrees with an earlier interpretation¹³ which argues that the $C-X$ and $D-X$ transitions which have been mentioned in the literature^{4,8,48} are actually part of the $B-X$ band system. Finally, numerous higher-lying excited states have also been found to possess well-defined minima, and a number of their radiative lifetimes are calculated to fall in the 1–20 ns region.

ACKNOWLEDGMENTS

One of us (A.B.A.) would like to thank the Alexander von Humboldt Foundation for the granting of a stipend. This work was supported in part by the Deutsche Forschungsgemeinschaft in the form of a Forschergruppe grant and within the Schwerpunktprogramm "Theorie relativistischer Effekte in der Chemie und Physik schwerer Elemente." The financial support of the Fonds der Chemischen Industrie is also hereby gratefully acknowledged.

¹W. C. Stwalley, J. Chem. Phys. **63**, 3062 (1975).

²J. M. Eder and E. Valenta, Denkschr. Wien Akad. **61**, 401 (1894).

³E. Hulthén, Z. Phys. **32**, 32 (1925); **50**, 319 (1928).

⁴R. Rydberg, Z. Phys. **73**, 74 (1931); **80**, 514 (1933).

⁵Y. Fujioka and Y. Tanaka, Sci. Pap. Inst. Phys. Chem. Res. Tokyo **34**, 713 (1938).

⁶T. L. Porter, J. Opt. Soc. Am. **52**, 1206 (1962).

- ⁷T. L. Porter and S. P. Davis, *J. Opt. Soc. Am.* **53**, 338 (1963).
- ⁸J. G. Phillips and S. P. Davis, *Berkeley Analyses of Molecular Spectra* (University of California, Berkeley, 1968).
- ⁹D. M. Eakin and S. P. Davis, *J. Mol. Spectrosc.* **35**, 27 (1970).
- ¹⁰O. Nedelec and J. Dufayard, *J. Chem. Phys.* **69**, 1833 (1978).
- ¹¹S. Mayama, S. Hiraoka, and K. Obi, *J. Chem. Phys.* **81**, 4760 (1984).
- ¹²J. Dufayard, B. Majournat, and O. Nedelec, *Chem. Phys.* **128**, 537 (1988).
- ¹³O. Nedelec, B. Majournat, and J. Dufayard, *Chem. Phys.* **134**, 137 (1989).
- ¹⁴R. S. Mulliken, *J. Phys. Chem.* **41**, 5 (1937).
- ¹⁵G. Herzberg, *Spectra of Diatomic Molecules* (Van Nostrand, Princeton, 1950), p. 425.
- ¹⁶L. Veseth, *J. Mol. Spectrosc.* **44**, 251 (1972).
- ¹⁷K. G. Dyall, K. Fægri, P. R. Taylor, and H. Partridge, *J. Chem. Phys.* **95**, 2583 (1991); K. G. Dyall, *ibid.* **96**, 1210 (1992).
- ¹⁸B. A. Hess, *Phys. Rev. A* **33**, 3742 (1986); G. Jansen and B. A. Hess, *Phys. Rev. A* **39**, 6016 (1989); R. Samzow and B. A. Hess, *Chem. Phys. Lett.* **184**, 491 (1991).
- ¹⁹M. Krauss and W. J. Stevens, *Annu. Rev. Phys. Chem.* **35**, 357 (1984); P. A. Christiansen, W. C. Ermler, and K. S. Pitzer, *ibid.* **36**, 407 (1985); O. Gropen, in *Methods in Computational Chemistry*, edited by S. Wilson (Plenum, New York, 1988), p. 109.
- ²⁰G. Das and A. Wahl, *J. Chem. Phys.* **64**, 4672 (1976).
- ²¹P. J. Hay, W. R. Wadt, L. R. Kahn, and F. W. Bobrowicz, *J. Chem. Phys.* **69**, 984 (1978).
- ²²A. Bernier, P. Millie, and M. Pelissier, *Chem. Phys.* **106**, 195 (1986).
- ²³M. Dolg, W. Küchle, H. Stoll, H. Preuss, and P. Schwerdtfeger, *Mol. Phys.* **74**, 1265 (1991).
- ²⁴U. Häussermann, M. Dolg, H. Stoll, H. Preuss, P. Schwerdtfeger, and R. M. Pitzer, *Mol. Phys.* **78**, 1211 (1993).
- ²⁵A. B. Alekseyev, R. J. Buenker, H.-P. Liebermann, and G. Hirsch, *J. Chem. Phys.* **100**, 2989 (1994).
- ²⁶A. B. Alekseyev, H.-P. Liebermann, I. Boustani, G. Hirsch, and R. J. Buenker, *Chem. Phys.* **173**, 333 (1993).
- ²⁷A. B. Alekseyev, H.-P. Liebermann, R. J. Buenker, G. Hirsch, and Y. Li, *J. Chem. Phys.* **100**, 8956 (1994).
- ²⁸K. K. Das, H.-P. Liebermann, R. J. Buenker, and G. Hirsch, *J. Chem. Phys.* **102**, 4518 (1995).
- ²⁹A. B. Alekseyev, K. K. Das, H.-P. Liebermann, R. J. Buenker, and G. Hirsch, *Chem. Phys.* **198**, 333 (1995).
- ³⁰Y. Li, H.-P. Liebermann, G. Hirsch, and R. J. Buenker, *J. Mol. Spectrosc.* **165**, 219 (1994).
- ³¹C. H. Teichteil, M. Pelissier, and F. Spiegelmann, *Chem. Phys.* **81**, 274 (1983).
- ³²K. Balasubramanian and K. S. Pitzer, *Adv. Chem. Phys.* **67**, 287 (1987); K. Balasubramanian, *Chem. Rev.* **90**, 93 (1990).
- ³³I. Boustani, S. N. Rai, H.-P. Liebermann, A. B. Alekseyev, G. Hirsch, and R. J. Buenker, *Chem. Phys.* **177**, 45 (1993).
- ³⁴A. B. Alekseyev, H.-P. Liebermann, R. J. Buenker, and G. Hirsch, *J. Chem. Phys.* **102**, 2539 (1995).
- ³⁵K. K. Das, A. B. Alekseyev, H.-P. Liebermann, G. Hirsch, and R. J. Buenker, *Chem. Phys.* **196**, 395 (1995).
- ³⁶R. B. Ross, J. M. Powers, T. Atashroo, W. C. Ermler, L. A. LaJohn, and P. A. Christiansen, *J. Chem. Phys.* **93**, 6654 (1990).
- ³⁷T. H. Dunning, Jr., *J. Chem. Phys.* **35**, 716 (1971).
- ³⁸R. J. Buenker and S. D. Peyerimhoff, *Theor. Chim. Acta* **35**, 33 (1974); **39**, 217 (1975); R. J. Buenker, S. D. Peyerimhoff, and W. Butscher, *Mol. Phys.* **35**, 771 (1978).
- ³⁹E. R. Davidson, in *The World of Quantum Chemistry*, edited by R. Daudel and B. Pullman (Reidel, Dordrecht, 1974), p. 17.
- ⁴⁰G. Hirsch, P. J. Bruna, S. D. Peyerimhoff, and R. J. Buenker, *Chem. Phys. Lett.* **52**, 442 (1977).
- ⁴¹R. J. Buenker, D. B. Knowles, S. N. Rai, G. Hirsch, K. Bhanuprakash, and J. R. Alvarez-Collado, in *Studies in Physical and Theoretical Chemistry, Vol. 62, Quantum Chemistry—Basic Aspects, Actual Trends*, edited by R. Carbó (Elsevier, Amsterdam, 1989), p. 181; D. B. Knowles, J. R. Alvarez-Collado, G. Hirsch, and R. J. Buenker, *J. Chem. Phys.* **92**, 585 (1990).
- ⁴²R. J. Buenker and R. A. Philips, *J. Mol. Struct. Theochem.* **123**, 291 (1985).
- ⁴³J. W. Cooley, *Math. Comput.* **15**, 363 (1961).
- ⁴⁴M. Perić, R. Runau, J. Römelt, S. D. Peyerimhoff, and R. J. Buenker, *J. Mol. Spectrosc.* **166**, 251 (1994).
- ⁴⁵C. E. Moore, *Arch. U.S. Natl. Bur. Stand. No.* **467**, Vol. 3 (1971).
- ⁴⁶B. Huron, J. P. Malrieu, and P. Rangurel, *J. Chem. Phys.* **58**, 5745 (1973).
- ⁴⁷Programs MCDF and GRASP; cf. I. P. Grant, B. J. McKenzie, P. H. Norrington, D. Mayers, and N. C. Pyper, *Comput. Phys. Commun.* **21**, 207 (1980); B. J. McKenzie, I. P. Grant, and P. H. Norrington, *ibid.* **21**, 233 (1980); M. Dolg, modified version for pseudopotential calculations; K. G. Dyall, I. P. Grant, C. T. Johnson, F. A. Parpia, and E. P. Plummer, *Comput. Phys. Commun.* **55**, 425 (1989).
- ⁴⁸K. P. Huber and G. Herzberg, *Molecular Spectra and Molecular Structure, Vol. 4. Constants of Diatomic Molecules* (Van Nostrand Reinhold, Princeton, 1979).
- ⁴⁹J.-P. Gu, R. J. Buenker, G. Hirsch, and M. Kimura, *J. Chem. Phys.* **102**, 7540 (1995).
- ⁵⁰I. D. Petsalakis, G. Theodorakopoulos, and R. J. Buenker, *J. Chem. Phys.* **92**, 4920 (1990); A. B. Alekseyev, V. S. Ivanov, A. M. Pravilov, and O. D. Shestakov, *Chem. Phys.* **155**, 173 (1991).
- ⁵¹A. D. McLean, *J. Chem. Phys.* **79**, 3392 (1983).